Wide-angle X-ray Diffraction of Human Stratum Corneum: Effects of Hydration and Terpene Enhancer Treatment

P. A. CORNWELL, B. W. BARRY, C. P. STODDART AND J. A. BOUWSTRA*

*Postgraduate Studies in Pharmaceutical Technology, The School of Pharmacy, University of Bradford, Bradford BD7 1DP, UK, and
*Division of Pharmaceutical Technology, Center for Bio-Pharmaceutical Sciences, University of Leiden, PO Box 9502, 2300 RA Leiden,
The Netherlands*

Abstract—Wide-angle X-ray-diffraction experiments were used to investigate the molecular organization of barrier components of human stratum corneum. Diffraction lines related to the side-by-side lipid packing arrangements in the intercellular bilayers were identified as were patterns arising from secondary protein structures in intracellular keratin. Reflections were also identified which may be produced by proteins in the corneocyte envelopes. The effects of hydration on stratum corneum structure were monitored using 0, 20–40, 40–60, 60–80 and approximately 300% hydrated samples. The packing arrangements in the intercellular lipid bilayers remained the same over the entire hydration range, as did keratin structures. A new diffraction ring, attributable to liquid water, was produced by 300% hydrated samples with a repeat spacing of 0·35 to 0·30–0·29 nm. The effects of three terpene enhancers, (+)-limonene, nerolidol and 1,8-cineole, on stratum corneum structure were monitored. Treatment with each of the terpenes produced additional reflections which were attributed to the presence of the respective liquid enhancers within the stratum corneum. (+)-Limonene produced an additional reflection at 0·503–0·489 nm, nerolidol, an additional reflection at 0·486–0·471 nm and 1,8-cineole, an intense reflection at 0·583–0·578 nm. Reflections characteristic of gel-phase lipids and crystalline lipids also remained after all terpene treatments. These results provide no clear evidence of lipid bilayer disruption by the terpenes and suggest that areas of liquid terpene exist within the stratum corneum. The mechanisms underlying propylene glycol synergy with terpene enhancers were investigated. Treatment of stratum corneum with each terpene mixed with propylene glycol gave rise to two additional reflections. One reflection, always positioned at 0·452–0·448 nm, had been observed in control studies following propylene glycol treatment and may have been associated with bilayer structures disrupted by propylene glycol or altered keratin structures. The second reflection was developed by the respective terpene enhancer. For example, treatment with a 1,8-cineole/propylene glycol mixture produced reflections at 0·457–0·451 nm (propylene glycol-disrupted lipids or altered keratin) and 0·591–0·578 nm (liquid 1,8-cineole). Since the reflection at 0·452–0·448 nm was unaffected by co-application of propylene glycol with terpene enhancers, this study offers no evidence to support the theory that propylene glycol synergy with the terpenes occurs through enhanced lipid disruption.

The outermost layer of the skin, the stratum corneum, is the rate limiting barrier to the percutaneous absorption of most drugs (Blank 1953; Monash & Blank 1958; Scheuplein 1965). The tissue consists of dead, flattened cells, filled with keratin, embedded in a lipid matrix (Elias et al 1977; Grayson & Elias 1982). The intercellular lipid accounts for 5–30% of the total tissue volume (Elias & Leventhal 1979). Lipids in the intercellular spaces are arranged in bilayer structures which run mainly parallel to the skin surface (Breathnach et al 1973; Elias & Friend 1975; Madison et al 1987). Drugs applied to the skin mainly partition into and diffuse through the stratum corneum via either a transcellular route or a much more tortuous intercellular pathway. For each route, the structural organization of the stratum corneum dictates that permeants must diffuse across the intercellular lipid bilayers.

The excellent barrier properties of human skin limit the range of drugs which can be administered transdermally. In order to promote drug delivery, investigators have sought to increase skin permeability using chemical enhancers. Skin penetration enhancers can act by disrupting lipid or protein

structures in the stratum corneum, or by improving drug partitioning into the skin (Barry 1988).

Many studies have shown that skin occlusion, leading to raised stratum corneum hydration, increases skin permeability to a wide range of drugs (Barry 1983). However, the precise mechanisms by which water increases the permeability of the stratum corneum have remained unclear. Differential scanning calorimetry (DSC) studies on human stratum corneum showed that increased hydration reduces the transition mid-point temperatures of both lipid and protein endotherms (Goodman & Barry 1989). The endotherm shifts were interpreted to mean that water increases intercellular lipid bilayer disorder and also loosens the structure of intracellular keratin. Recent investigations, however, have called these interpretations into question. Small-angle X-ray diffraction (XRD) studies on human stratum corneum suggested that the intercellular lipid bilayers do not swell between 6 and 150% w/w hydration (using the definition of percent hydration used in the present study) (Bouwstra et al 1991a). In good agreement with these studies, wide-angle XRD determinations suggested no change in lipid or protein organization between hydration levels of 6 and 67% w/w (Bouwstra et al 1992). In addition, Fourier transform infrared spectroscopy measurements using perdeuterated

Correspondence: B. W. Barry, Postgraduate Studies in Pharmaceutical Technology, The School of Pharmacy, University of Bradford, Bradford BD7 1DP, UK.

water illustrated that the proportion of gauche acyl chain conformers in human stratum corneum lipids does not change between hydration levels of 0 and 35% w/w (Mak et al 1991). Lipid bilayer order, and thus permeability is, therefore, unlikely to change significantly between these hydration levels.

It is possible that the lack of structural changes observed on hydration may relate to the relatively restricted hydration ranges arbitrarily selected by investigators. The level of hydration obtained in-vivo following skin occulation for an extended time will be much higher than 150% w/w. In the present study, therefore, the effects of almost full hydration (approx. 300% w/w) on skin structure were investigated using wide-angle XRD.

Terpenes, isolated from natural essential oils, are currently under investigation as safe, non-irritant skin penetration enhancers (Williams & Barry 1990; Cornwell & Barry 1991). Mono- and sesquiterpene compounds have been shown to act, at least in part, by increasing the apparent drug diffusivity in the stratum corneum (Cornwell & Barry 1991; Williams & Barry 1991). DSC and small-angle XRD studies suggest that terpene enhancers may increase drug diffusivity by disrupting the intercellular lipid bilayers (Williams & Barry 1989; Cornwell et al 1993). Recent skin electrical conductivity measurements have also shown that terpene enhancer treatment increases the permeability of the stratum corneum to ions (Cornwell & Barry 1993). A correlation between increased ion transport and 5-fluorouracil penetration suggests that terpene enhancers may create polar pathways across the stratum corneum through which ions and polar drugs may pass. The precise locations of the polar pathways have, to date, remained unclear. It has been suggested, however, that they are likely to reside in the intercellular lipid bilayers.

In the present study we investigated the effects of terpene enhancers on the structure of human stratum corneum using wide-angle XRD. The terpenes (+)-limonene, nerolidol and 1,8-cineole, were applied to stratum corneum samples for 12 h as undiluted oils and as solutions in propylene glycol.

In-vitro permeation studies, using the model hydrophilic permeant, 5-fluorouracil, have shown there is synergistic effect between terpenes and propylene glycol (Barry & Williams 1989). Small-angle XRD experiments suggest that the synergy may arise through increased lipid disruption (Cornwell et al 1993). The molecular mechanism by which propylene glycol exerts this effect was also investigated in the present study.

Materials and Methods

Human skin samples
Human abdominal mid-line skin samples were obtained post-mortem and stored on receipt at −20°C in double-sealed evacuated polythene bags (Harrison et al 1984). Samples from eleven donors were used. The sex and age of each of the donors were as follows: donor I, female, 88; donor II, male, 74; donor III, male, 60; donor IV, female, 72; donor V, female, 86; donor VI, male, 69; donor VII, male, 82; donor VIII, female, 82; donor IX, female, 78; donor X, female, 63; donor XI, male, 39.

Isolation of stratum corneum
Epidermal membranes were prepared by immersing full thickness skin samples, trimmed of subcutaneous fat tissue, in water at 60°C for 45 s, after which the epidermis could be gently peeled off the underlying dermis (Kligman & Christophers 1963). The stratum corneum was isolated by floating the heat-separated epidermal membranes on an aqueous solution of 0·0001% trypsin (Sigma Chemical Co., St Louis, USA) and 0·5% sodium bicarbonate for 12 h. Digested material was removed from the underside of the stratum corneum with tissue paper and the prepared sheets were rinsed in an aqueous solution of 0·002% sodium azide. Cleaned sheets were dried on PTFE-coated wire meshes under ambient conditions. Each sheet was rinsed in acetone for 20 s to remove any sebaceous or subcutaneous fat contamination, and stored for a maximum of two weeks over silica-gel under vacuum.

Preparation of stratum corneum for XRD measurements
Before the XRD experiments, dried stratum corneum sheets were cut into 10–15 mg samples, and hydrated over a saturated aqueous solution of potassium sulphate (relative humidity = 97% at 25°C). The majority of samples were hydrated to between 20 and 40% hydration, where the percentage hydration was defined as:

$$\text{Percentage hydration} = \frac{\text{wet weight} - \text{dry weight}}{\text{dry weight}} \quad (1)$$

To identify which diffraction lines were associated with lipid structures in the stratum corneum, lipid-extracted tissue was analysed. Lipids were extracted by immersing stratum corneum samples in a chloroform:methanol (2:1) mixture for a minimum of 48 h (Bligh & Dyer 1959); samples were rehydrated to 20–40% hydration before X-ray analysis. The effectiveness of the extraction procedure was checked by subjecting portions of the extracted samples to DSC. The absence of lipid-based endotherms confirmed that the procedure removed most of the free lipid in the stratum corneum.

For hydration studies, samples were prepared to 0, 20–40, 40–60, 60–80 and approximately 300% hydration. Between 20 and 80% hydration, stratum corneum samples were conditioned over a saturated aqueous solution of potassium sulphate. To achieve 300% hydration, samples were floated on an aqueous solution of 0·002% sodium azide for 48 h.

In enhancer experiments, 20–40% hydrated stratum corneum samples were treated for 12 h with terpene oils or terpenes in propylene glycol. The 12-h treatment time was chosen to mimic the treatment period used in previous in-vitro permeation studies (Cornwell & Barry 1991; Williams & Barry 1991). A similar 12-h treatment was also used in recent small-angle XRD experiments (Cornwell et al 1993), which allows direct comparison of data.

The enhancers investigated were (+)-limonene and 1,8-cineole (Sigma Chemical Co., St Louis, USA; monoterpenes) and nerolidol (mixture of isomers, Aldrich Gillingham, UK; sesquiterpene). Scheme 1 illustrates their molecular structures and space-filling models. Gas chromatographic analysis has shown each of the terpenes to be > 99% pure. For the propylene glycol studies, (+)-limonene

and 1,8-cineole were applied as saturated solutions in propylene glycol and nerolidol (which was completely miscible with propylene glycol) was applied as a 90% w/w solution in propylene glycol. The terpene/propylene glycol mixtures were identical to those used in previous small-angle XRD experiments (Cornwell et al 1993), permitting direct comparison of data. Each enhancer experiment was performed in duplicate using samples of stratum corneum obtained from two different skin donors.

All prepared samples were transported to the Daresbury Laboratory in hermetically sealed DSC pans (internal volume $75\,\mu L$). The pans were opened in a small vice immediately before X-ray analysis. Changes in sample hydration and evaporation of volatile enhancer oils were therefore kept to a minimum.

Wide-angle XRD measurements

Wide-angle XRD experiments were performed at the Daresbury Laboratory (Cheshire, UK) using the Synchrotron Radiation Source (SRS). Experiments were performed at Station 7·2 using the fibre camera. The source radiation was focused in the vertical plane by a bent, fused silica mirror. The beam was monochromated using a 20 cm long bent triangular [111]Ge crystal with a 10·4° asymmetric cut. The monochromator was adjusted to produce a beam wavelength (λ) of 0·1488 nm (calibrated with pure Ni foil). After passing through a final collimeter, placed between the end of the beam-line and the sample, the beam had a diameter, in the focal plane, of $0·3\,mm^2$. When the SRS is running at 2 GeV and 250 mA, the intensity of the beam is estimated to be approximately 2×10^{10} photons s^{-1}.

Diffraction patterns were recorded on Reflex 25 X-ray films (Cea AB, Sweden). Two films were sandwiched in each cartridge to improve the range of reflection intensities which could be detected. Measurements were made over two beam-time periods. The sample-to-film distance (L) during the first experimental period was 77·7 mm and in the second period was 67·8 mm. Teflon tape was used as a standard (major d-spacings; 0·486 and 0·288 nm) with which to calculate L. In this study reflections over a 2θ range of approximately 3 to 45° were recorded, i.e. first-order d-spacings of between 2·8 nm and 0·19 nm.

Stratum corneum samples were mounted, randomly orientated, into sealed sample holders with thin mica windows. The beam path length through the samples was 1 mm. Samples were exposed to the beam for approximately 15 min at room temperature (21°C).

Results

The origins of the diffraction patterns arising from untreated stratum corneum

Control diffraction patterns were collected from stratum corneum samples obtained from eight different skin donors (Table 1). The intensities of the diffraction lines produced by different samples varied considerably. In some instances only the most intense reflections were detected (for example, the control pattern obtained from stratum corneum from donor VII). Similar variability has been reported in other wide-angle XRD studies using human stratum corneum (Garson et al 1991; Bouwstra et al 1992). In

contrast to intensities, reflection positions were remarkably consistent. The minor variations in reflection positions mainly arise from unavoidable experimental error, i.e. very small changes in the sample-to-film distance and errors in the manual measurement of the diffraction ring diameters on the photographic film.

Lipid-based reflections

Common to all untreated samples were two sharp and intense reflections at 0·416–0·412 and 0·374–0·371 nm (Fig. 1a). These reflections have been reported in previous wide-angle XRD studies using human callous (Swanbeck 1959), human stratum corneum (Wilkes et al 1973a; Garson et al 1991; Bouwstra et al 1992) and murine stratum corneum (Elias et al 1983; White et al 1988). They have been shown to be associated with lipid bilayer structures located in the intercellular spaces (Elias et al 1983; White et al 1988; Garson et al 1991). Diffraction lines at both 0·416–0·412 and 0·374–0·371 nm are characteristically produced by crystalline lipids with an orthorhombic perpendicular alkyl chain packing arrangement (Small 1986). However, a single line at 0·416–0·412 nm is also characteristic of gel phase lipids with a slightly looser hexagonal alkyl-chain packing arrangement (Small 1986). It is possible, therefore, that both crystalline and gel phase lipids may coexist in the stratum corneum, i.e. there may be lateral phase separation in the bilayers. It should be stressed that these experiments were performed at room temperature (21°C). Other wide-angle XRD studies on murine and human stratum corneum have shown that gel phase lipids with an hexagonal packing arrangement predominate above the first lipid phase transition at 35–36°C (White et al 1988; Bouwstra et al 1992).

Lipid extraction with chloroform : methanol removed the 0·374–0·371 nm spacing but only diminished the intensity of the 0·416–0·412 nm reflection (Table 1). Similar observations have been reported by Bouwstra et al (1992). It is possible that the 0·416–0·412 nm reflection produced by lipid-extracted tissue may arise from lipids covalently bound to the corneocyte envelope (Swartzendruber et al 1987; Wertz et al 1989). Bound lipids account for 1·4% of dry tissue weight of human stratum corneum (Wertz et al 1989) which corresponds to approximately 10% of total stratum corneum lipids, assuming free lipids make up 5–15% of dry tissue weight (Wilkes et al 1973b). To confirm the hypothesis that bound lipids produce a weak reflection at 0·416–0·412 nm, X-ray analyses could be repeated using lipid-extracted tissue from which the bound lipids had been removed from the corneocyte envelopes by hydrolysis of the ester linkages. Unfortunately, restricted beam-time did not allow for such an experiment in the present study.

In addition to the strong reflections at 0·416–0·412 and 0·374–0·371 nm, many samples produced a medium or weak intensity diffraction line at 0·304–0·303 nm. This reflection was not produced by lipid-extracted samples and is thus likely to be associated with lipid packing arrangements. A similar reflection has also been reported by Garson et al (1991) and Bouwstra et al (1992).

Some samples developed sharp diffraction lines located at 0·575–0·572, 0·514, 0·503 and 0·489–0·486 nm. Similar

Table 1. Summary of wide-angle X-ray diffraction patterns obtained from untreated human stratum corneum.

			Reflection position (nm)/intensity							Interpretation
			20–40% Hydrated samples					Delipidized samples		
Donor I	Donor II	Donor III	Donor IV	Donor V	Donor VI	Donor VII	Donor X	Donor VIII	Donor VII	
2·27 (w)		2·27 (s)	2·27 (s)					2·21 (w)		Higher order reflections from large lipid bilayer spacings (see text)
		1·66 (w)	1·57 (w)							
	1·37 (vw)	1·42 (m)	1·41 (m)				1·40 (w)	1·37 (w)		
		1·17 (w)	1·16 (w)					1·13 (w)		
1·2–0·87 (w,d)	1·2–0·87 (m,d)		?–0·87 (w,d)	1·1–0·89 (m,d)	1·2–0·89 (w,d)	1·1–0·89 (w,d)	1·1–0·89 (w,d)	?–0·87 (w,d)	1·1–0·89 (m,d)	Soft keratin
				0·926 (m,sp)				0·916 (vw,sp)		Corneocyte envelope (?)
	0·572 (m)			0·575 (m)						Crystalline cholesterol
0·51–? (w,d)	0·52–0·35 (m,d)	0·52–? (w,d)	0·52–0·43 (w,d)	0·52–0·34 (m,d)	0·52–0·39 (w,d)	0·52–0·39 (w,d)	0·52–0·36 (w,d)	0·52–0·38 (w,d)	0·52–0·36 (m,d)	Soft keratin
	0·514 (w)									Crystalline cholesterol
	0·503 (w)									Crystalline cholesterol
0·489 (w)	0·484 (m)	0·489 (m)		0·486 (m)	0·486 (m)		0·486 (m)			Crystalline cholesterol
				0·452 (m,sp)				0·451 (w,sp)		Corneocyte envelope (?)
0·412 (s)	0·412 (s)	0·412 (s)	0·416 (s)	0·416 (s)	0·412 (s)	0·412 (s)	0·412 (s)	0·412 (w)	0·416 (w)	Crystalline/ gel phase lipids
0·372 (m)	0·371 (s)	0·373 (s)	0·373 (m)	0·374 (m)	0·374 (m)	0·371 (m)	0·374 (m)			Crystalline lipids
				0·312 (m,sp)				0·309 (vw,sp)		Corneocyte envelope (?)
			0·303 (w)	0·303 (m)	0·304 (w)		0·303 (w)			Crystalline lipids (?)
				0·262 (w,sp)						Corneocyte envelope (?)
				0·257 (w,sp)						Corneocyte envelope (?)
	0·245 (vw)		0·249 (w)	0·247 (m,sp)	0·249 (vw)		0·249 (vw)	0·245 (vw,sp)		Corneocyte envelope (?)
0·230 (w)	0·230 (s,sp)	0·230 (s,sp)	0·230 (s,sp)	0·220 (vw,sp)				0·230 (m,sp)		Corneocyte envelope (?)

? = reflection edge not clear or not visible. vw = very weak intensity, w = weak, m = medium, s = strong. Most reflections were smooth and sharp. However, some were diffuse (d) or speckled (sp).

diffraction lines have been reported in previous studies on human stratum corneum (Garson et al 1991; Bouwstra et al 1992). Bouwstra et al (1992) suggest that the reflections arise from crystalline cholesterol. This is reasonable since the reflections are absent in lipid-extracted tissue and since anhydrous cholesterol produces intense reflections at 0·574, 0·523, 0·508 and 0·490 (De Wolff 1989). Stratum corneum lipids contain approximately 20% cholesterol (Elias 1990) some of which could conceivably phase-separate within the bilayers. It is interesting to note that small-angle XRD studies on human stratum corneum have detected a reflection at 3·35 nm which may also be related to crystalline cholesterol (Bouwstra et al 1991a).

Finally, some control samples produced a series of sharp diffraction lines close to the beam stop, at 2·27, 1·66–1·57, 1·42–1·37 and 1·17–1·16 nm. These reflections probably represent higher-order reflections from large lipid bilayer spacings. Previous small-angle XRD studies have shown that two unit cells exist in human stratum corneum bilayers; a 6·4 and a 13·4 nm unit cell (Bouwstra et al 1991a; Cornwell et al 1993). It is difficult to index the reflections observed in the present study to one or the other unit cell. The strong reflection at 2·27 nm may be either a sixth-order reflection from a 13·6 nm unit cell or a third-order reflection from a

6·8 nm unit cell, or a combination of both. The diffraction line at 1·66–1·57 nm may be either an eighth-order reflection from a 13·0 nm unit cell, or a fourth-order reflection from a 6·5 nm unit cell, or it may be due to crystalline cholesterol which produces a strong reflection at 1·62 nm (De Wolff 1989). The 1·42–1·37 nm reflection could be either a tenth-order reflection from a 14·0 nm unit cell or a fifth-order reflection from a 7·0 nm unit cell, or a combination of the two. Finally, the 1·17–1·16 nm reflection may represent a twelfth-order reflection from a 14·0 nm unit cell or a sixth-order reflection from a 7·0 nm unit cell, or a combination of the two.

Keratin-based reflections

The majority of untreated stratum corneum samples produced two broad and diffuse reflections at 1·2–1·1 to 0·89–0·87 nm and 0·52–0·51 to 0·43–0·34 nm which are characteristic of epidermal keratin. Diffuse reflections attributed to soft keratin, centred at 0·98 and 0·46 nm, have been reported in many other wide-angle XRD studies using human stratum corneum (Wilkes et al 1973a; Garson et al 1991; Bouwstra et al 1992).

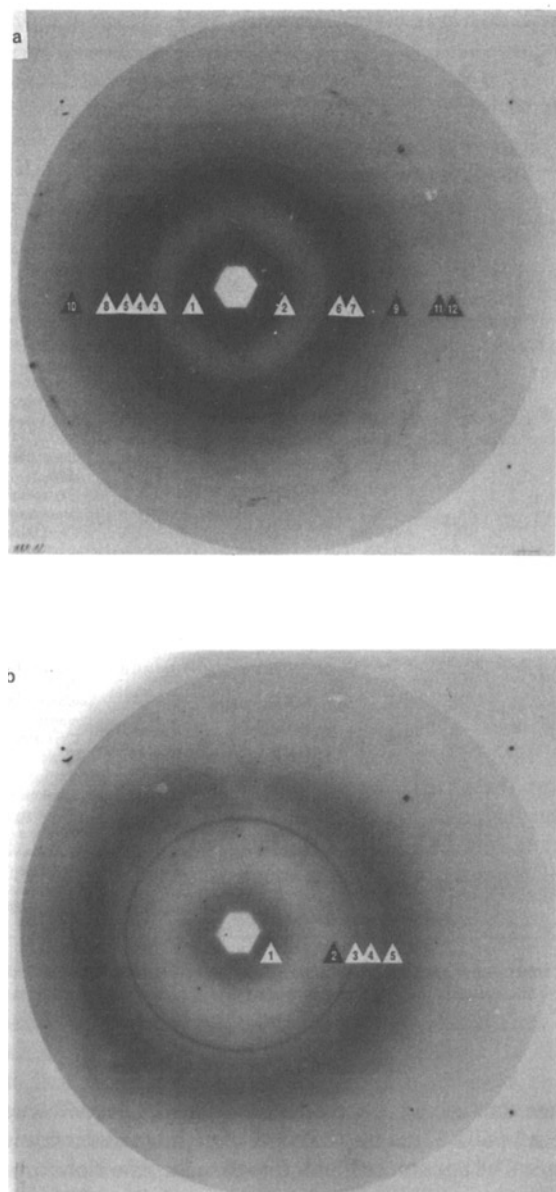Much evidence (mainly biochemical) has accumulated which suggests that epidermal keratin comprises mainly

FIG. 1. a. Wide-angle X-ray diffraction pattern from untreated 20–40% hydrated stratum corneum; donor V. The diffraction lines arrowed are: $1 = 1\cdot1-0\cdot89$ nm, $2 = 0\cdot926$ nm, $3 = 0\cdot575$ nm, $4 = 0\cdot486$ nm, $5 = 0\cdot52-0\cdot34$ nm, $6 = 0\cdot452$ nm, $7 = 0\cdot416$ nm, $8 = 0\cdot374$ nm, $9 = 0\cdot312$ nm, $10 = 0\cdot303$ nm, $11 = 0\cdot257$ nm, $12 = 0\cdot220$ nm. b. Diffraction pattern from approximately 300% hydrated stratum corneum; donor X. The diffraction lines arrowed are: $1 = ?-0\cdot93$ nm, $2 = 0\cdot52-?$ nm, $3 = 0\cdot412$ nm, $4 = 0\cdot374$ nm, $5 = 0\cdot35-0\cdot30$ nm. (The sample-to-film distance for both measurements was $67\cdot8$ mm). ? = reflection edge not clear or not visible.

α-helix protein (Steinert & Cantieri 1983). This evidence implies that epidermal keratin filaments are built from a super-coil of nine sub-units and that each sub-unit consists of a triplet of coiled α-helices. Direct evidence of α-helix keratin obtained in-situ for human stratum corneum has been recorded using Fourier transform infrared spectroscopy (Oertel 1977) and Fourier transform Raman spectroscopy (Williams et al 1992).

The keratin pattern observed in the present study does not clearly indicate the presence of α-keratin. The diffuse reflections at $1\cdot2-1\cdot1$ to $0\cdot89-0\cdot87$ nm and $0\cdot51$ to $0\cdot43-0\cdot34$ nm are most characteristic of amorphous keratin.

The X-ray diffraction pattern characteristic of α-keratin in, for example, mammalian hair is very well defined (Mercer 1961). One normally expects a sharp line at $0\cdot51$ nm (the so-called axial repeat spacing), a strong, diffuse reflection at approximately $1\cdot0$ nm and a strong, diffuse reflection at approximately $0\cdot42$ nm. In agreement with this pattern, diffuse reflections centred at approximately $1\cdot0$ and $0\cdot45$ nm were observed in the present study. However, the characteristic α-keratin reflection at $0\cdot51$ nm was not resolved.

Closer examination of the diffuse reflection centred at approximately $0\cdot45$ nm reveals some evidence in favour of the presence of α-keratin. The sharply defined inside edge at $0\cdot52-0\cdot51$ nm may arise from the characteristic α-keratin diffraction line at $0\cdot51$ nm which is unresolved from the main reflection (Fig. 1a).

Garson et al (1991) argue that the soft keratin pattern produced by human stratum corneum loosely resembles that of β-keratin. By means of densitometry those authors located diffuse maxima at $0\cdot96$ and $0\cdot93$ nm which are at a slightly different location from that expected for α-keratin ($0\cdot98$ nm) and which match unit cell dimensions for a form of β-keratin. Most importantly, however, the absence of a clear α-keratin reflection at $0\cdot51$ nm was taken as strong evidence in favour of the β-form.

Overall, it can be concluded that the X-ray diffraction pattern produced by intracellular keratin is too weak and diffuse to index to a particular secondary protein structure. The reflections observed relate most closely to those produced by amorphous keratin. However, the presence of α-keratin cannot be excluded.

Reflections from the corneocyte envelope

The diffraction pattern obtained from stratum corneum from donor V featured sharp, speckled reflections at $0\cdot926$, $0\cdot452$, $0\cdot312$, $0\cdot262$, $0\cdot257$, $0\cdot247$ and $0\cdot220$ nm (Fig. 1a, Table 1). Many other control patterns also contained sharp, speckled reflections at $0\cdot249-0\cdot245$ and $0\cdot230-0\cdot220$ nm. Similar reflections at $0\cdot916$, $0\cdot451$, $0\cdot309$, $0\cdot245$ and $0\cdot230$ nm were also observed in lipid-extracted tissue obtained from donor VIII.

The sharpness of the diffraction lines and their speckled nature (which presumably arises from individual crystallites within the samples) both suggest that the structures to which they are linked are highly crystalline. The production of such reflections by lipid-extracted tissue further suggests that they are protein based.

It is possible that these reflections arise from the corneocyte envelopes. Sharp, smooth diffraction lines at $0\cdot94$ and $0\cdot46$ nm were reported by White et al (1988) using murine stratum corneum. The reflections remained in lipid-extracted tissue, in agreement with the results of the present study, and were also observed in membrane couplet preparations devoid of intracellular material. The authors suggested that the reflections may arise from the β-pleated protein believed to be present in the corneocyte envelope.

Contrary to these observations Garson et al (1991) reported that human stratum corneum produces reflections at $0\cdot94$, $0\cdot47$ and $0\cdot315$ nm which are not present in mem-

brane couplet preparations. Those authors argue that the reflections arise, not from the corneocyte envelopes, but possibly from intracellular proteins.

Effects of hydration and terpene enhancers on the diffraction patterns

In this study the overall intensities of the diffraction patterns and the relative intensities of specific diffraction lines were affected by the stratum corneum sample used, the SRS beam intensity during the measurement, the exposure time, the film sensitivity and slight variations in the film processing and development procedure. It is, therefore, difficult to interpret changes in intensities of particular reflections following a specific treatment. Only qualitative interpretations of the new diffraction lines are thus attempted.

Effects of hydration on the diffraction patterns

Diffraction patterns were collected from stratum corneum samples prepared at five different hydration levels; 0, 20–40, 40–60, 60–80 and approximately 300% hydrated (Tables 1, 2).

No major changes in lipid-chain packing were observed over the entire hydration range. The intense reflections at 0·416–0·412 and 0·374–0·368 nm were clearly visible at all hydration levels. The overall intensity and resolution of the diffraction patterns appeared to decrease with increasing water content of the sample so that at high hydration levels some weaker lipid-based reflections were no longer visible. Such reductions in reflection intensities were probably due to the absorption of X-rays by water in the samples. Water is

well known as a strong X-ray absorber. There was no evidence to suggest that the disappearance of these weak diffraction lines at high hydration levels was due to changes in lipid packing.

The soft keratin pattern weakened in intensity on hydration but did not change (Tables 1,2). The normal pattern, with reflections at 1·2–1·1 to 0·89–0·87 nm and 0·52–0·51 to 0·43–0·34 nm was produced by all samples between 0 and approximately 300% hydration. At approximately 300% hydration a new, diffuse reflection at 0·35 to 0·30–0·29 nm was observed (Fig. 1b). Subsequent analysis of liquid water revealed that this reflection could be attributed to water in the stratum corneum (water reflection was at 0·32 nm).

Effects of terpene penetration enhancers on the diffraction patterns

After 12-h treatment with undiluted terpene enhancer oils, stratum corneum samples continued to produce strong reflections at 0·416–0·406 and 0·376–0·368 nm (Fig. 2, Table 3). This suggests that parts of the intercellular lipid domains are unaffected by enhancer treatment. Presumably, the Van der Waals' forces of attraction between these lipid chains are sufficiently strong to prevent significant numbers of terpene molecules penetrating between them at ambient temperatures. In agreement with this concept, when a molten mixture of octadecanol (selected as a simple model lipid) and 1,8-cineole was cooled to room temperature (21°C), the mixture solidified and most of the terpene separated as droplets.

Table 2. Effects of hydration on the wide-angle X-ray diffraction patterns obtained from human stratum corneum.

	Reflection position (nm)/intensity						Interpretation
	Dry samples			40–60% hydrated sample	60–80% hydrated sample	Approximately 300% hydrated samples	
Donor II	Donor IX	Donor X	Donor X	Donor X	Donor IX	Donor X	
1·96 (s)							Higher order reflections from large lipid bilayer spacings (see text)
1·37 (w)							
1·22 (m)							
0·99 (w)							
?–0·87 (w,d)	1·1–0·89 (w,d)	1·1–0·89 (w,d)	1·1–0·89 (w,d)	1·1–0·89 (w,d)	?–0·97 (w,d)	?–0·93 (w,d)	Soft keratin
0·565 (m)							Crystalline cholesterol
0·52–0·38 (w,d)	0·52–0·42 (w,d)	0·52–0·39 (w,d)	0·52–0·36 (w,d)	0·52–0·34 (w,d)	0·52–? (vw,d)	0·52–? (vw,d)	Soft keratin
0·480 (m)		0·492 (m)	0·486 (m)	0·486 (w)			Crystalline cholesterol
0·412 (s)	0·412 (s)	0·412 (s)	0·412 (s)	0·416 (s)	0·416 (s)	0·412 (s)	Crystalline/gel phase lipids
0·368 (m)	0·371 (m)	0·374 (m)	0·374 (m)	0·374 (m)	0·374 (w)	0·374 (w)	Crystalline lipids
					0·35–0·29 (w,d)	0·35–0·30 (w,d)	Water
		0·323 (vw,sp)					Corneocyte envelope (?)
	0·303 (w)	0·304 (w)	0·303 (w)	0·303 (m)	0·303 (m)		Crystalline lipids (?)
0·247 (vw,sp)		0·249 (vw,sp)					Corneocyte envelope (?)
0·230 (s,sp)							Corneocyte envelope (?)

? = reflection edge not clear or not visible. vw = very weak intensity, w = weak, m = medium, s = strong. Most reflections were smooth and sharp. However, some were diffuse (d) or speckled (sp).
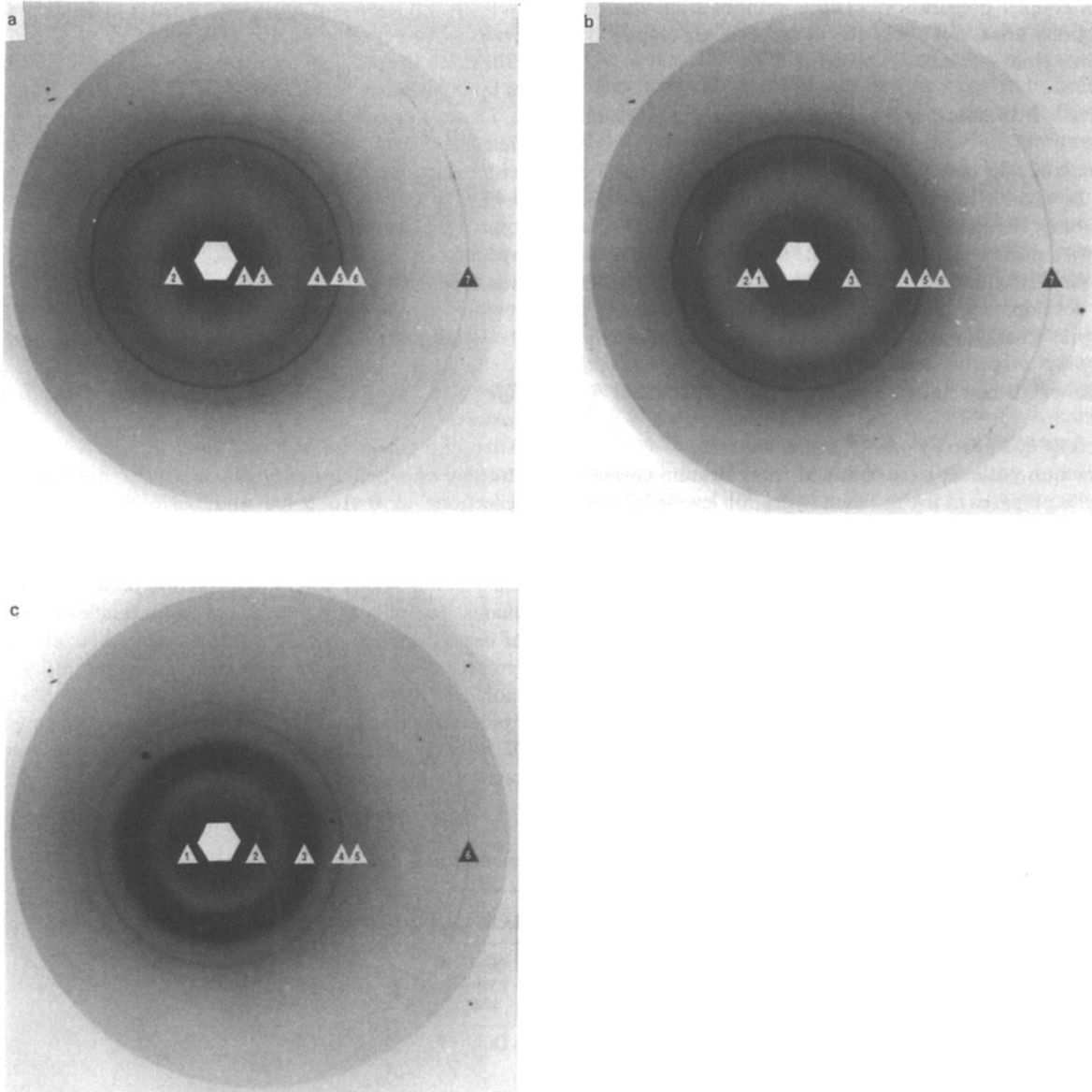
FIG. 2. a. Wide-angle X-ray diffraction pattern from stratum corneum pretreated with neat (+)-limonene; donor XI. The diffraction lines arrowed are: $1 = 1\cdot37$ nm, $2 = 1\cdot13$ nm, $3 = ?-0\cdot87$ nm, $4 = 0\cdot489$ nm, $5 = 0\cdot409$ nm, $6 = 0\cdot368$ nm, $7 = 0\cdot230$ nm. b. Diffraction pattern from stratum corneum pretreated with neat nerolidol; donor XI. The diffraction lines arrowed are: $1 = 1\cdot22$ nm, $2 = 0\cdot97$ nm, $3 = ?-0\cdot87$ nm, $4 = 0\cdot471$ nm, $5 = 0\cdot406$ nm, $6 = 0\cdot368$ nm, $7 = 0\cdot230$ nm. c. Diffraction pattern from stratum corneum pretreated with neat 1,8-cineole; donor XI. The diffraction lines arrowed are: $1 = 1\cdot33$ nm, $2 = ?-0\cdot90$ nm, $3 = 0\cdot578$ nm, $4 = 0\cdot412$ nm, $5 = 0\cdot373$ nm, $6 = 0\cdot230$ nm. The sample-to-film distance for all three measurements was $77\cdot7$ mm. ? = reflection edge not clear or not visible.

After terpene treatment additional reflections appeared on the diffraction patterns. (+)-Limonene treatment produced a diffuse reflection at 0·503–0·489 nm, nerolidol treatment a diffuse reflection at 0·486–0·471 nm and 1,8-cineole treatment an intense, diffuse reflection at 0·583–0·578 nm. In the case of nerolidol and 1,8-cineole these reflections could be attributed to the liquid enhancers which, in control experiments employing the SRS, produced reflections at 0·48 and 0·58 nm, respectively. In further control experiments, employing a regular laboratory diffractometer (Cu Kα radiation (45 kV, 50 mA), pinhole collimator, evacuated camera, film detection, exposure time of 72 h), neat (+)-limonene produced a very weak, diffuse reflection at approximately 0·50 nm. The new reflection observed in (+)-limonene-treated stratum corneum is, thus, also likely to be associated with the presence of liquid enhancer within the samples. Why terpenes should produce a diffraction pattern in their liquid state is not clear and requires further investigation.

Previous small-angle XRD studies on human stratum corneum have shown that 12-h treatment with either (+)-limonene or 1,8-cineole markedly reduces the periodicity of the intercellular lipid bilayers (Cornwell et al 1993). The reduction in periodicity could be ascribed to a disrup-

Table 3. Effects of terpene enhancer treatment on the wide-angle X-ray diffraction patterns obtained from human stratum corneum.

Reflection position (nm)/intensity						Interpretation
(+)-Limonene treated		Nerolidol treated		1,8-Cineole treated		
Donor V	Donor XI	Donor V	Donor XI	Donor V	Donor XI	
	2·27 (s)					
	1·60 (w)	1·96 (s)			1·60 (m)	Higher order reflections from large lipid bilayer spacings (see text)
	1·37 (m)	1·37 (w)			1·33 (m)	
	1·13 (w)	1·22 (m)				
		0·97 (w)				
1·1–0·89 (w,d)	?–0·87 (w,d)	?–0·89 (w,d)	?–0·87 (w,d)	1·1–0·89 (w,d)	?–0·90 (w,d)	Soft keratin
0·926 (m,sp)		0·926 (m,sp)				Corneocyte envelope (?)
				0·583 (s,d)	0·578 (s,d)	Liquid 1,8-cineole / Soft keratin
0·503 (m,d)	0·489 (m,d)	0·52–0·39 (w,d)				Liquid (+)-limonene
		0·486 (m,d)	0·471 (m,d)			Liquid nerolidol
0·457 (m,sp)		0·488 (w,sp)		0·457 (w,sp)		Corneocyte envelope (?)
0·452 (m,sp)						Corneocyte envelope (?)
0·416 (s)	0·409 (s)	0·412 (s)	0·406 (s)	0·416 (s)	0·412 (s)	Crystalline/gel phase lipids
0·376 (m)	0·368 (m)	0·371 (m)	0·368 (m)	0·376 (m)	0·373 (m)	Crystalline lipids
0·313 (m,sp)		0·312 (w,sp)		0·313 (vw,sp)		Corneocyte envelope (?)
0·312 (m,sp)						Corneocyte envelope (?)
0·304 (vw)		0·301 (w)		0·304 (w)		Crystalline lipids (?)
0·264 (w,sp)		0·260 (w,sp)		0·262 (w,sp)		
0·261 (w,sp)						
0·247 (m,sp)	0·247 (vw,sp)	0·247 (m,sp)		0·247 (m,sp)		Corneocyte envelope (?)
0·220 (vw,sp)	0·230 (m,sp)		0·230 (m,sp)		0·230 (m,sp)	
0·210 (vw,sp)						

? = reflection edge not clear or not visible. vw = very weak intensity, w = weak, m = medium, s = strong. Most reflections were smooth and sharp. However, some were diffuse (d) or speckled (sp).

tion of the stacking arrangement of the bilayers or to a disordering of the lipid packing within the bilayers or to both.

Closer examination of the diffraction patterns produced by (+)-limonene- and 1,8-cineole-treated samples from donor XI, reveals small-angle reflections attributable to lipid bilayer spacings (N.B. treated samples from donor V show no such reflections). This was unexpected since small-angle XRD studies have shown that both enhancers almost completely abolish small-angle reflections (Cornwell et al 1993). This inconsistency may be explained on the basis of inter-individual variability. It is possible that lipid bilayer periodicity in samples from donor XI is relatively resistant to enhancer effects. Unfortunately, due to restrictions on beam-time, this could not be investigated further.

Small-angle XRD experiments have also shown that 12-h treatment with nerolidol slightly increases lipid bilayer periodicity (Cornwell et al 1993). The increase in periodicity was postulated to arise from lateral bilayer expansion associated with the insertion of the long-chain alcohol enhancer into the lipid bilayers. (The sesquiterpene nerolidol, with its extended alkyl chain and a polar hydroxyl

group, has a structure suitable for alignment within lipid bilayers, unlike (+)-limonene and 1,8-cineole; see Scheme 1.) The results of the present study provide no evidence that nerolidol treatment produces new lipid bilayer structures. Further investigation is necessary to see if nerolidol produces laterally expanded bilayers within the stratum corneum.

This study has shown that, after terpene enhancer treatment, both normal bilayers (i.e. gel phase and crystalline lipids) and areas of liquid enhancer co-exist in the stratum corneum. The consequences of this for drug diffusion are discussed later.

Effects of terpene penetration enhancers dissolved in propylene glycol on the diffraction patterns

Following 12-h propylene glycol application, a new medium intensity diffraction line at 0·452–0·448 nm appeared, whilst strong reflections at 0·416–0·412 and 0·376–0·371 nm, characteristic of normal (gel phase and crystalline) lipids, remained (Fig. 3, Table 4). The new reflection does not arise from liquid propylene glycol which in control experiments
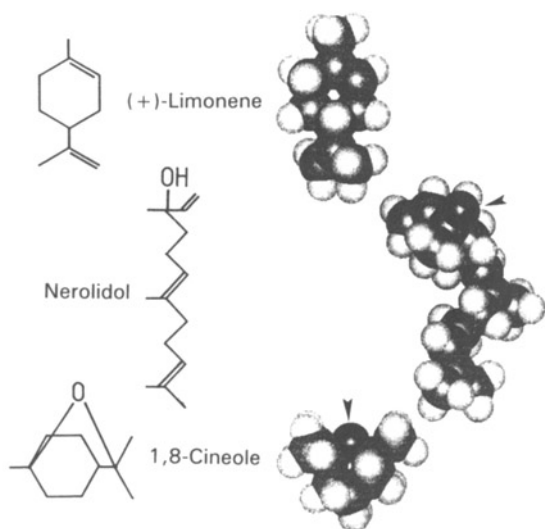
SCHEME 1. Molecular structures and space-filling (3D) models of the terpenes (+)-limonene, nerolidol and 1,8-cineole. Oxygen atoms are marked with an arrow head. Space-filling models were developed using the HyperChem computational chemistry approach. The option used for minimizing the charge distribution was the AM1 semi-empirical method; geometry optimization employed the MM + approach.

produced no coherent scatter. Instead it may be associated with a new, looser, lipid packing arrangement or with an altered keratin structure. It is interesting to note that the spacing (0·452–0·448 nm) is very close to the spacing reported in liquid crystalline lipid bilayers above their phase transition temperatures of 0·46 nm (Wilkes et al 1973a; White et al 1988; Bouwstra et al 1992). It is postulated that propylene glycol may compete with water of hydration at bilayer/water interfaces and disrupt normal lipid head-group packing, thus increasing lipid alkyl-chain disorder within the bilayers. These data suggest that propylene glycol treatment gives rise to regions of disrupted lipids which coexist with normal lipid bilayers.

Small-angle XRD studies on human stratum corneum have shown that lipid bilayer repeat distances do not change following propylene glycol treatment (Bouwstra et al 1991b; Cornwell et al 1993). This observation suggests that propylene glycol is able to disrupt the lipid bilayers whilst leaving their overall bilayer structure intact. Bouwstra et al (1991b) argue that propylene glycol can be positioned between lipid headgroups, thus disrupting lipid packing within the bilayer but not changing overall bilayer thickness.

It is equally possible that the reflection at 0·452–0·448 nm arises from altered keratin structures. This would be in agreement with the results of DSC investigations which suggest that propylene glycol acts to expand and to solvate intracellular keratin structures, thereby promoting trans-cellular drug diffusion (Barry 1987).

After treatment with terpenes dissolved in propylene glycol, each stratum corneum sample produced two new reflections. For example, tissue exposed to 1,8-cineole saturated in propylene glycol developed new reflections at 0·457–0·451 and 0·591–0·578 nm (Fig. 3, Table 4). The 0·457–0·451 nm reflection can be ascribed to propylene glycol-disrupted lipids or altered keratin structures (char-

acteristic spacing = 0·452–0·448 nm) and the 0·591–0·578 nm reflections to liquid 1,8-cineole (characteristic spacing = 0·583–0·578 nm). Samples treated with (+)-limonene or nerolidol in propylene glycol produced new, overlapping, reflections at 0·451–0·448 and 0·52–0·51 to 0·46–0·42 nm. The 0·451–0·448 nm reflections can again be linked to propylene glycol-disrupted lipid structures or altered keratin structures (characteristic spacing = 0·452–0·448 nm) and the diffuse 0·52–0·51 to 0·46–0·42 nm reflections to liquid (+)-limonene or liquid nerolidol (characteristic spacings = 0·503–0·489 and 0·486–0·471 nm for (+)-limonene and nerolidol, respectively).

Sharp reflections at 0·416–0·409 and 0·374–0·371 nm, associated with normal (gel phase or crystalline) lipid bilayers, were observed in all samples treated with terpene/propylene glycol mixtures. This study suggests, therefore, that samples treated with terpene/propylene glycol mixtures may contain a minimum of three lipid phases: normal lipid bilayers, areas of liquid terpene and possibly propylene glycol-disrupted lipid bilayers.

It has been shown that propylene glycol synergistically improves the activities of terpene penetration enhancers (Barry & Williams 1989). Small-angle XRD studies on human stratum corneum have shown that monoterpene/propylene glycol mixtures reduce lipid bilayer periodicity more than do the respective terpene enhancers alone (Cornwell et al 1993). Since propylene glycol had a limited effect on bilayer periodicity itself, it was suggested that propylene glycol synergy occurs through a potentiation of the lipid disruptive effects of the monoterpenes. In the present study no evidence of such a specific potentiation effect was observed. The reflection positioned at 0·452–0·448 nm was not affected by the presence of the terpenes, thus indicating no synergy between propylene glycol and the enhancers. Clearly, more work is required to uncover the actual mechanisms underlying propylene glycol synergy. However, it is important to note that the experiments and data considered in the present paper and the relevant quoted references are concerned essentially with the effects of the terpenes on lipid and protein structures within the stratum corneum. No consideration is given here to the effects of the enhancers on the solubilities of drugs within separate domains in the stratum corneum, nor to the subsequent modifications to micro-partition coefficients between these regions. Such effects may be at least as important for the enhancement of polar drug permeation as the alterations in microstructure considered here.

Discussion

The lipid-protein-partitioning concept of enhancer action suggests that skin penetration enhancers act by disrupting lipid or protein structures in the stratum corneum, or by improving drug partitioning into the tissue or between microdomains within the horny layer (Barry 1988). The results of the present study suggest that water does not act to disrupt the intercellular lipids or the intracellular keratin. No changes in the lipid reflections or the keratin pattern were observed between 80 and 300%-hydration. The swelling of the corneocytes under such hydration may induce fractures in the intercellular lipid domain leading to increased permeation
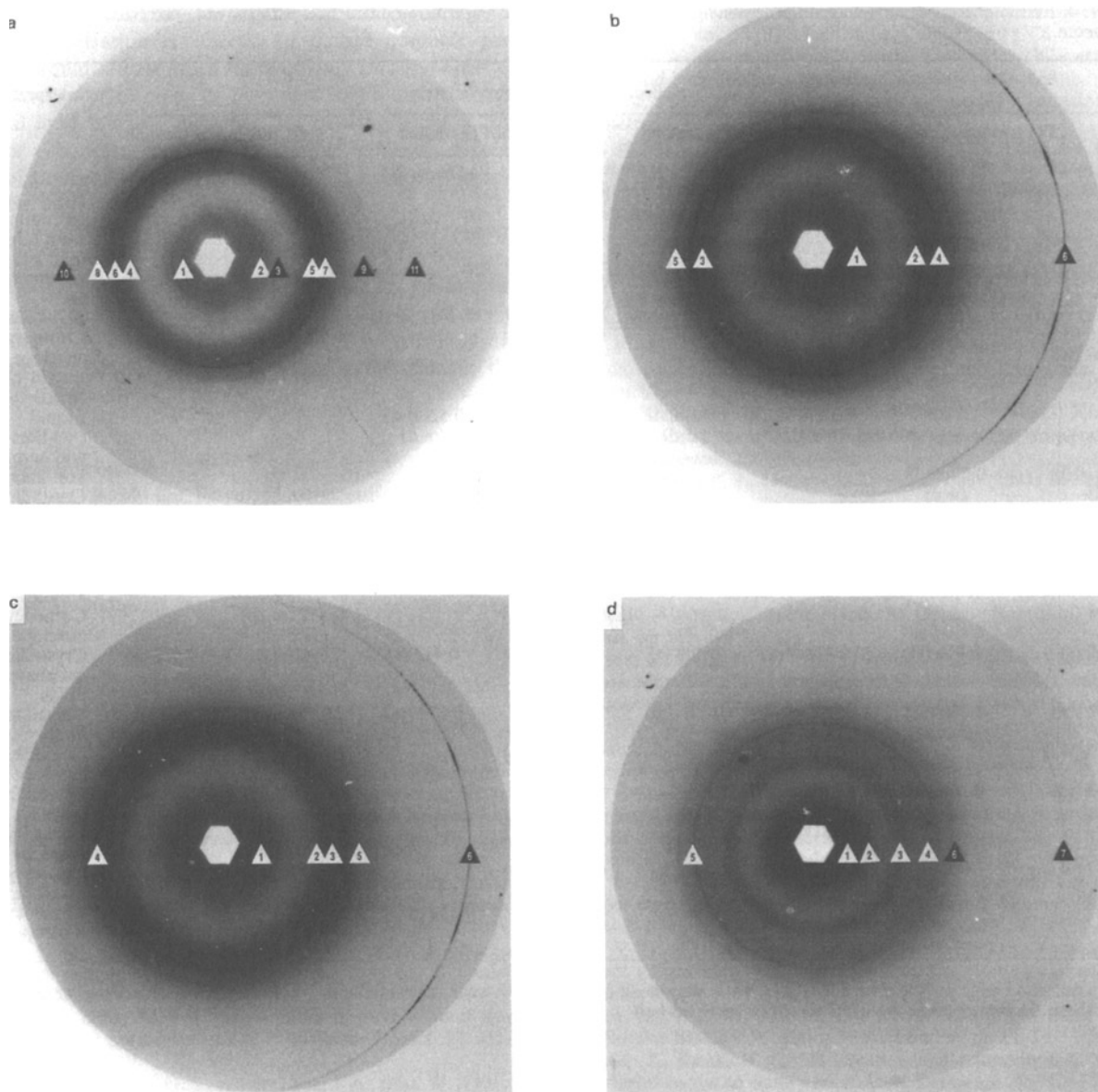
FIG. 3. a. Wide-angle X-ray diffraction pattern from stratum corneum pretreated with propylene glycol; donor V. The diffraction lines arrowed are: 1 = ?–0·89 nm, 2 = 0·926 nm, 3 = 0·708 nm, 4 = 0·486 nm, 5 = 0·448 nm, 6 = 0·52–0·38 nm, 7 = 0·412 nm, 8 = 0·371 nm, 9 = 0·310 nm, 10 = 0·303 nm, 11 = 0·247 nm. b. Diffraction pattern from stratum corneum pretreated with (+)-limonene saturated in propylene glycol; donor XI. The diffraction lines arrowed are: 1 = ?–0·87 nm, 2 = 0·52–0·42 nm, 3 = 0·451 nm, 4 = 0·409 nm, 5 = 0·371 nm, 6 = 0·230 nm. c. Diffraction pattern from stratum corneum pretreated with nerolidol (90% w/w) in propylene glycol; donor XI. The diffraction lines arrowed are: 1 = ?–0·87 nm, 2 = 0·52–0·43 nm, 3 = 0·451 nm, 4 = 0·412 nm, 5 = 0·373 nm, 6 = 0·230 nm. d. Diffraction pattern from stratum corneum pretreated with 1,8-cineole saturated in propylene glycol; donor XI. The diffraction lines arrowed are: 1 = 1·45 nm, 2 = ?–0·90 nm, 3 = 0·578 nm, 4 = 0·451 nm, 5 = 0·412 nm, 6 = 0·371 nm, 7 = 0·230 nm. The sample-to-film distance for measurement a was 67·8 mm, the distance for measurements b–d was 77·7 mm. ? = reflection edge not clear or not visible.

of molecules through the stratum corneum via these micro-shunt routes.

The present study has not provided any direct evidence of intercellular lipid bilayer disruption by the terpenes. This may be because bilayer disruption is only associated with a decrease in intensity in the reflections arising from the gel phase and crystalline lipids. Changes in reflection intensity between different samples could not be measured quantitatively in this study. The possibility that terpene enhancers

disrupt the intercellular lipid bilayers thus cannot be ruled out.

Reflections attributed to liquid enhancers were produced by stratum corneum samples treated with neat terpene oils and terpene/propylene glycol mixtures. These data are in agreement with terpene enhancer uptake studies which have shown that large amounts of terpene exist within human stratum corneum following a 12 h treatment period in-vitro (Cornwell 1993). Enhancer uptake values, as a percentage of

Table 4. Effects of terpene enhancers in propylene glycol (PG) on the wide-angle X-ray diffraction patterns obtained from human stratum corneum.

Reflection position (nm)/intensity								Interpretation
PG treated		(+)-Limonene/PG treated		Nerolidol/PG treated		1,8-Cineole/PG treated		
Donor V	Donor IV	Donor V	Donor XI	Donor V	Donor XI	Donor V	Donor XI	
							1·45 (w)	Higher order reflection from large lipid bilayer spacing (see text)
?–0·89 (w,d) 0·926 (m,sp) 0·708 (w)	?–0·93 (w,d)	?–0·89 (w,d) 0·926 (m,sp)	?–0·87 (w,d)	?–0·89 (w,d) 0·926 (m,sp)	?–0·87 (w,d)	0·926 (m,sp)	?–0·90 (w,d)	Soft keratin Corneocyte envelope (?)
						0·591 (s,d)	0·578 (m,d)	Liquid 1,8-cineole
		0·51–0·42 (m,d)	0·52–0·42 (m,d)	0·52–0·46 (m,d)	0·52–0·43 (m,d)			Liquid (+)-limonene and nerolidol
0·52–0·38 (w,d) 0·486 (m)	0·52–0·38 (w,d)							Soft keratin Crystalline cholesterol (?)
0·448 (m)	0·452 (m)	0·448 (m)	0·451 (m,d)	0·448 (m)	0·451 (m,d)	0·457 (m)	0·451 (w,d)	Disrupted lipids or altered keratin
0·448 (m,sp)		0·448 (m,sp)		0·448 (m,sp)		0·457 (m,sp)		Corneocyte envelope (?)
0·412 (s)	0·416 (s)	0·416 (s)	0·409 (s)	0·416 (s)	0·412 (s)	0·416 (s)	0·412 (s)	Crystalline/gel phase lipids
0·371 (m)	0·376 (m)	0·374 (m)	0·371 (m)	0·374 (m)	0·373 (m)	0·376 (m)	0·371 (m)	Crystalline lipids
0·310 (w,sp)		0·312 (m,sp)		0·312 (w,sp)		0·312 (w,sp)		Corneocyte envelope (?)
0·303 (m)	0·306 (w)	0·303 (m)		0·304 (m)		0·304 (m)		Crystalline lipids (?)
		0·260 (vw,sp)		0·260 (w,sp)		0·262 (vw,sp)		Corneocyte envelope (?)
0·247 (w,sp)		0·247 (w,sp)	0·247 (vw)	0·247 (m,sp)		0·247 (w,sp)		Corneocyte envelope (?)
			0·230 (m,sp)		0·230 (m,sp)		0·230 (m,sp)	Corneocyte envelope (?)

? = reflection edge not clear or not visible. vw = very weak intensity, w = weak, m = medium, s = strong. Most reflections were smooth and sharp. However, some were diffuse (d) or speckled (sp).

dry tissue weight, obtained following treatment with neat (+)-limonene, nerolidol and 1,8-cineole were; 8·90, 39·6 and 26·2%, respectively.

Since the terpenes under study are lipophilic, it is likely they distribute preferentially into the intercellular spaces of the stratum corneum. We can postulate, therefore, that areas of liquid enhancer may coexist alongside normal (gel phase and crystalline) bilayers. It should be noted, however, that although the terpenes may not partition strongly into the aqueous interiors of the corneocytes, the higher volume of the intracellular spaces relative to the intercellular domain means that a significant amount of terpene may also be present within the corneocytes.

Studies on model lipid membranes have shown that ion transport is relatively unaffected by lipid viscosity, but may increase markedly at the gel to liquid-crystalline phase transition temperature, where lateral phase separation is believed to occur (Deamer & Bramhall 1986). The boundaries between the two lipid phases are believed to form ion-permeable pathways. It is interesting to note that terpene enhancer treatment increases the permeability of the

stratum corneum to ions (Cornwell & Barry 1993). It is possible that the different lipid domains suggested by the present study may give rise to boundary regions which are permeable to ions.

The suggestion that domain-boundaries can enhance transport for ionic species across the stratum corneum is not new. Fourier transform infrared spectroscopy measurements have shown the coexistence of fluid oleic acid and ordered intercellular lipids in porcine stratum corneum (Ongpipattanakul et al 1991). The authors suggest that the boundary regions between the two phases may allow enhanced passage of ionically-charged molecules.

The importance of the postulated permeable boundary regions in promoting the absorption of un-ionized drugs is not clear. Increases in ion permeability produced by different terpene treatments have been directly related to increases in the rate of absorption of the model polar drug 5-fluorouracil (Cornwell & Barry 1993). It is possible, therefore, that permeable boundary regions could promote both ion transport and the absorption of polar non-electrolytes. The production of such permeable pathways through the

intercellular lipids may be one mechanism of action for terpene penetration enhancers. Of course nonionic permeants would diffuse much more quickly through areas of liquid enhancer or areas of disrupted lipids than through normal lipid bilayers, all other things being equal. Thus, terpene enhancers would act via two mechanisms—formation of permeable boundary regions and provision of less resistive lipid routes.

Finally, the mechanisms behind propylene glycol synergy have not been fully resolved in this study. Further experiments utilizing DSC and measuring terpene uptake into the stratum corneum, with and without propylene glycol, are in progress. The mechanisms underlying propylene glycol synergy will be discussed in a future publication in the light of these additional data.

References

Barry, B. W. (1983) Dermatological Formulations: Percutaneous Absorption. Marcel Dekker, New York and Basel

Barry, B. W. (1987) Mode of action of penetration enhancers in human skin. J. Contr. Rel. 6: 85–97

Barry, B. W. (1988) Action of skin penetration enhancers—the lipid-protein-partitioning theory. Int. J. Cosmet. Sci. 10: 281–293

Barry, B. W., Williams, A. C. (1989) Human skin penetration enhancement: the synergy of propylene glycol with terpenes. Proc. Int. Symp. Contr. Rel. Bioact. Mater. 16: 33–34

Blank, I. H. (1953) Further observations on factors which influence the water content of the stratum corneum. J. Invest. Dermatol. 21: 259–269

Bligh, E. G., Dyer, W. J. (1959) A rapid method of total lipid extraction and purification. Can. J. Biochem. Physiol. 37: 911–917

Bouwstra, J. A., Gooris, G. S., van der Spek, J. A., Bras, W. (1991a) Structural investigations of human stratum corneum by small angle X-ray scattering. J. Invest. Dermatol. 97: 1005–1012

Bouwstra, J. A., de Vries, M. A., Gooris, G. S., Bras, W., Brussee, J., Ponec, M. (1991b) Thermodynamic and structural aspects of the skin barrier. J. Contr. Rel. 15: 209–220

Bouwstra, J. A., Gooris, G. S., Salomons-de Vries, M. A., van der Spek, J. A., Bras, W. (1992) Structure of human stratum corneum as a function of temperature and hydration: a wide-angle X-ray diffraction study. Int. J. Pharm. 84: 205–216

Breathnach, A. S., Goodman, C., Stoliski, C., Gros, M. (1973) Freeze-fracture replication of cells of stratum corneum of human epidermis. J. Anat. 114: 65–81

Cornwell, P. A. (1993) Mechanisms of Action of Terpene Penetration Enhancers in Human Skin. PhD Thesis, University of Bradford, UK

Cornwell, P. A., Barry, B. W. (1991) Determination of the mode of action of sesquiterpene skin penetration enhancers. J. Pharm. Pharmacol. 43 (Suppl.): 56P

Cornwell, P. A., Barry, B. W. (1993) The routes of penetration of ions and 5-fluorouracil across human skin and the mechanisms of action of terpene skin penetration enhancers. Int. J. Pharm. 94: 189–194

Cornwell, P. A., Bouwstra, J. A., Gooris, G. S., Barry, B. W. (1993) Small-angle X-ray diffraction investigations of terpene enhancer actions on the lipid barrier in human skin. In: Brain, K. R.,

James, V. J., Walters, K. A. (eds) Predictions of Percutaneous Penetration. Vol. 3b, STS Publishing, Cardiff, pp 18–26

Deamer, D. W., Bramhall, J. (1986) Permeability of lipid bilayers to water and ionic solutes. Chem. Phys. Lipids 40: 167–188

De Wolff, P. M. (1989) X-ray diffraction pattern for anhydrous cholesterol. JCPDS Database, Pattern 7-742

Elias, P. M. (1990) The importance of epidermis lipids for the stratum corneum barrier. In: Osborne, D., Amann, A. (eds) Topical Drug Delivery Formulations. Marcel Dekker, New York and Basel, pp 13–28

Elias, P. M., Friend, D. S. (1975) The permeability barrier in mammalian epidermis. J. Cell. Biol. 65: 180–191

Elias, P. M., Leventhal, M. E. (1979) Intercellular volume changes and cell surface expansion during cornification. Clin. Res. 27: 525a

Elias, P. M., Goerke, J., Friend, D. S. (1977) Permeability barrier lipids; composition and influence on epidermal structure. J. Invest. Dermatol. 69: 535–546

Elias, P. M., Bonar, L., Grayson, S., Baden, H. P. (1983) X-ray diffraction analyses of stratum corneum membrane couplets. J. Invest. Dermatol. 80: 213–214

Garson, J., Doucet, J., Lévêque, J., Tsoucaris, G. (1991) Oriented structure in human stratum corneum revealed by X-ray diffraction. J. Invest. Dermatol. 96: 43–49

Goodman, M., Barry, B. W. (1989) Action of penetration enhancers on human stratum corneum as assessed by differential scanning calorimetry. In: Bronaugh, R. L., Maibach, H. I. (eds) Percutaneous Absorption. 2nd edn, Marcel Dekker, New York and Basel, pp 567–593

Grayson, S., Elias, P. M. (1982) Isolation and lipid biochemical characterisation of stratum corneum membrane complex: implications for the cutaneous permeability barrier. J. Invest. Dermatol. 78: 128–135

Harrison, S. M., Barry, B. W., Dugard, P. H. (1984) Effects of freezing on human skin permeability. J. Pharm. Pharmacol. 36: 261–262

Kligman, A. M., Christophers, E. (1963) Preparations of isolated sheets of human stratum corneum. Arch. Dermatol. 88: 70–73

Madison, K. C., Swartzendruber, D. C., Wertz, P. W., Downing, D. T. (1987) Presence of intact intercellular lipid lamellae in the upper layers of the stratum corneum. J. Invest. Dermatol. 88: 714–718

Mak, V. H. W., Potts, R. O., Guy, R. H. (1991) Does hydration affect intercellular lipid organisation in the stratum corneum? Pharm. Res. 8: 1064–1065

Mercer, E. H. (1961) Keratin and Keratinisation: An Essay in Molecular Biology. Pergamon Press, London, pp 14–15

Monash, S., Blank, H. (1958) Location and reformation of the epithelial barrier to water vapor. Arch. Dermatol. 78: 710–714

Oertel, R. P. (1977) Protein conformational changes induced in human stratum corneum by organic sulphoxides: an infra-red spectroscopic investigation. Biopolymers 16: 2329–2345

Ongpipattanakul, B., Burnette, R. R., Potts, R. O., Francoeur, M. L. (1991) Evidence that oleic acid exists in a separate phase within stratum corneum lipids. Pharm. Res. 8: 350–354

Scheuplein, R. J. (1965) Mechanism of percutaneous absorption. I. Routes of penetration and the influence of solubility. J. Invest. Dermatol. 45: 334–346

Small, D. M. (1986) The physical chemistry of lipids: from alkanes to phospholipids. Handbook of Lipid Research, Volume 4, Plenum Press, New York, pp 43–87

Steinert, P. M., Cantieri, J. S. (1983) Epidermal keratins. In: Goldsmith, L. A. (ed.) Biochemistry and Physiology of the Skin. Volume 1, Oxford University Press, New York and Oxford, pp 135–169

Swanbeck, G. (1959) Macromolecular organisation of epidermal keratin: an X-ray diffraction study of the horny layer from normal, ichthyotic and psoriatic skin. Acta Derm. Venereol. 39 (Suppl. 43): 5–37

Swartzendruber, D. C., Wertz, P. W., Madison, K. C., Downing, D. T. (1987) Evidence that the corneocyte has a chemically bound lipid envelope. J. Invest. Dermatol. 88: 709–713

Wertz, P. W., Swartzendruber, D. C., Kitko, D., Madison, K. C., Downing, D. T. (1989) The role of the corneocyte lipid envelopes

in cohesion of the stratum corneum. J. Invest. Dermatol. 93: 169–172

White, S. H., Mirejovsky, D., King, G. I. (1988) Structure of lamellar lipid domains and corneocyte envelopes of murine stratum corneum. An X-ray diffraction study. Biochemistry 27: 3725–3732

Wilkes, G. L., Brown, I. A., Wildnauer, R. H. (1973a) Structure-property relations of human and neonatal rat stratum corneum. I. Thermal stability of the crystalline lipid structure as studied by X-ray diffraction and differential thermal analysis. Biochim. Biophys. Acta 304: 267–275

Wilkes, G. L., Brown, I. A., Wildnauer, R. H. (1973b) The biomechanical properties of skin. Crit. Rev. Bioeng. 1: 453–495

Williams, A. C., Barry, B. W. (1989) Permeation, FTIR and DSC investigations of terpene penetration enhancers in human skin. J. Pharm. Pharmacol. 41 (Suppl.): 12P

Williams, A. C., Barry, B. W. (1990) The use of terpenes as skin penetration enhancers. In: Scott, R. C., Guy, R. H., Hadgraft, J. (eds) Prediction of Percutaneous Penetration. Vol. 2, IBC Technical Services, London, pp 224–230

Williams, A. C., Barry, B. W. (1991) Terpenes and the lipid-protein-partitioning theory of skin penetration enhancement. Pharm. Res. 8: 17–24

Williams, A. C., Edwards, H. G. M., Barry, B. W. (1992) Fourier transform Raman spectroscopy. A novel application for examining human stratum corneum. Int. J. Pharm. 81: R11–R14